DUAL BRAIDS AND THE BRAID ARRANGEMENT

par

Jon McCammond

Résumé. — The braid groups have several well-known classifying spaces. There is a classical classifying space derived from the complement of the complex braid arrangement, which, when viewed as a complexification of the real braid arrangement, is closely related to the Salvetti complex, the standard Artin presentation and the standard Garside structure of the braid group. The dual presentation of the braid group, introduced by Birman, Ko and Lee in 1998, leads to a second Garside structure and a second piecewise Euclidean classifying space that my co-authors and I call the dual braid complex with the orthoscheme metric. Since both sequences of spaces are classifying spaces for the same sequence of groups, they are homotopy equivalent. Recently, Michael Dougherty and I have been able to made the connection between these two spaces much more concrete using a natural embedding of the dual braid complex into the corresponding quotient of the complex braid arrangement complement. This homotopy equivalent subspace is defined by viewing the points in the classical classifying space as polynomials. In fact, this approach leads to several new metric complexes, interesting combinatorics, and connections to other parts of the mathematics. In particular, we add a natural piecewise Euclidean metric and a cell structure to a compactification of the quotient of the classical classifying space. We call the result the *critical value complex* since the critical values of the polynomials labeling points are used to define both the metric and the cell structure. With this metric on the quotient of the classical classifying space, the embedding of the dual braid complex with the orthoscheme metric become an isometric embedding.

Dedicated to Ruth Charney on her birthday

The primary goal of this article is to draw attention to an emerging connection between two classifying spaces for the braid groups. On the one hand there is the classical classifying space which is a quotient of the complement of the complex braid arrangement. When viewed as a complexification of the real braid arrangement, this classifying space is closely related to the Salvetti complex, the standard Artin presentation and the standard Garside structure of the braid group [**Art25, Art47, Gar69, Sal87, Dav08, DDD+15**]. On the other hand, there is the dual presentation of the braid group, first introduced by Birman, Ko and Lee in 1998, which leads to a second Garside structure and a second piecewise Euclidean classifying space that my co-authors and I call the dual braid complex with the orthoscheme metric

[**BKL98, Bra01, Bes03, BM10, DMW20**]. Since both sequences of spaces are classifying spaces for the same sequence of groups, they are homotopy equivalent.

Recently, Michael Dougherty and I have been able to made the connection between these two spaces much more concrete in a series of articles. This article, which is both a survey of some results already available ([**DM20, DMa**]) and a research announcement of other results in preparation ([**DMb**]), closely follows the talk that I gave during the "CharneyFest" conference in Ohio. I have tried my best to preserve the many advantages of a live presentation, preserving the hand-drawn figures from my slides, keeping the language intentionally informal, and sweeping most of the details under the proverbial rug. As mentioned above, one goal is to try and make clear the results that Michael and I are proving and why they might be of interest. My other main goal is to advertise how we are using polynomials to establish the connection between these two sequences of spaces. I should also note that all of the new results described in this article are joint work wtih Michael Dougherty.

Structure of the Article. — The article is divided into four sections. Section 1 reviews the classical classifying space for the braid groups constructed as a quotient of the complex braid arrangement complement. Section 2 reviews the piecewise Euclidean classifying space constructed from the dual Garside structure that my co-authors and I call the dual braid complex with the orthoscheme metric. Section 3 describes the critical value complex and some of the theorems that this perspective allows us to establish between these two types of classifying spaces. And finally, Section 4 describes some of the ingredients that go into the proofs. In particular, for each individual complex polynomial with distinct roots, we construct a locally $\mathrm{CAT}(0)$ branched annulus with a metric rectangular tiling, and the way in which the structure and metric of these branched annuli vary as the polynomial varies, determines the metric and cell structure on the complex hyperplane complement.

1. The Braid Arrangement Complement

If V is a d-dimensional vector space with coordinates provided by a fixed ordered basis, then the symmetric group SYM_d acts on V by permuting these coordinates. Although this natural SYM_d-action is not free, the points with non-trivial stabilizers form a union of hyperplanes known as the braid arrangement.

***Definition 1.1.* —** The set of points in V where all coordinates are distinct can be described as the complement of a union of hyperplanes where some pair of coordinates are equal. Concretely, let $H_{ij} = \{\mathbf{z} \in V \mid z_i = z_j\}$ be the hyperplane where the i-th and j-th coordinates are equal, and let

$$\mathcal{H} = \bigcup_{i,j \in [d]} H_{ij}$$

be the union of these $\binom{d}{2}$ hyperplanes. The subset $\mathcal{H}$ is the *braid arrangement* and SYM_d acts freely on its complement, $V - \mathcal{H}$.

For vector spaces over $\mathbb{R}$ or $\mathbb{C}$, the only cases of interest here, V can be identified with $\mathbb{R}^d$ or $\mathbb{C}^d$. The symmetric group also acts on a lower dimensional space obtained by quotienting out the 1-dimensional subspace fixed by all of SYM_d.

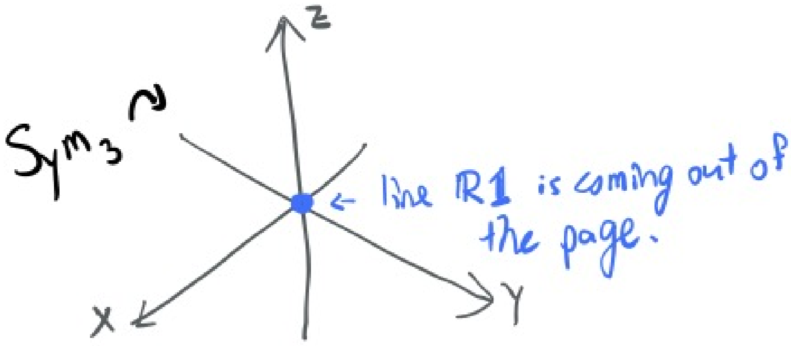

FIGURE 1. The 3-element symmetric group acts on $\mathbb{R}^3$ fixing the line $\mathbb{R}\mathbf{1}$ where all coordinates are equal. The action descends to the quotient space $\mathbb{R}^3/\mathbb{R}\mathbf{1} \cong \mathbb{R}^2$.

Remark 1.2. **—** If $\mathbf{1}$ denotes the vector with all coordinates equal to 1, then the line $\mathbb{R}\mathbf{1}$, respectively $\mathbb{C}\mathbf{1}$, is the 1-dimensional subspace where all coordinates are equal. This line is fixed pointwise under any permutation of coordinates and the SYM_d-action descends to the quotient vector space $\mathbb{R}^d/\mathbb{R}\mathbf{1}$, respectively $\mathbb{C}^d/\mathbb{C}\mathbf{1}$. Since all the hyperplanes in the braid arrangement $\mathcal{H}$ also contain this line, it also descends to the quotient. Figure 1 shows the SYM_3-action on $\mathbb{R}^3/\mathbb{R}\mathbf{1}$, along with the three lines in the braid arrangement quotient.

Remark 1.3. **—** The main space of interest is $Y = \text{SYM}_d\backslash(\mathbb{C}^d - \mathcal{H})/\mathbb{C}\mathbf{1}$. This is the lower dimensional version of the complex braid arrangement complement, where we also quotient by the free symmetric group action. In the natural metric coming from $\mathbb{C}$, this is a locally Euclidean, $(2d-2)$-dimensional open manifold without boundary, which is not compact and not complete. Michael Dougherty and I introduce an alternative, **bounded** metric on this space, defined using polynomials, so that its compact metric completion can be given the structure of a finite piecewise Eucldean, polyhedral cell complex. See Sections 3 and 4.

The connection between this space and the braid group can be seen via the standard configuration space trick. A single point in $\mathbb{C}^d$ can be viewed as d labeled points in $\mathbb{C}$, and a loop in $\mathbb{C}^d$ can be viewed as an d-strand pure braid. Similarly, a single point in $\mathbb{R}^d$ can be viewed as d labeled points in $\mathbb{R}$. See Figure 2.

Remark 1.4. **—** Using the configuration space trick, it is easy to see that $\pi_1(\mathbb{C}^d - \mathcal{H}) = \text{PBRAID}_d$ and $\pi_1(\text{SYM}_d\backslash(\mathbb{C}^d - \mathcal{H})/\mathbb{C}\mathbf{1}) = \text{BRAID}_d$. In particular, the removal of the braid arrangement $\mathcal{H}$ means labeled points in $\mathbb{C}$ are distinct, the quotient by SYM_d means labeled points become unlabeled, and the quotient by fixed line $\mathbb{C}\mathbf{1}$ simply means that point configurations are only considered up to rigidity translation. Tracing out the point configurations over time produces the (pure) braids. It has long been known that these spaces are classifying spaces for the pure braid groups and the braid groups [**BS72, Del72**].

Remark 1.5. **—** When working over the reals, the complement $\mathbb{R}^d - \mathcal{H}$ is disconnected with $d!$ connected components, freely permuted by SYM_d, and the quotient space $\text{SYM}_d\backslash(\mathbb{R}^d - \mathcal{H})$ is contractible. The cell structure dual to the real braid arrangement is a Euclidean polytope

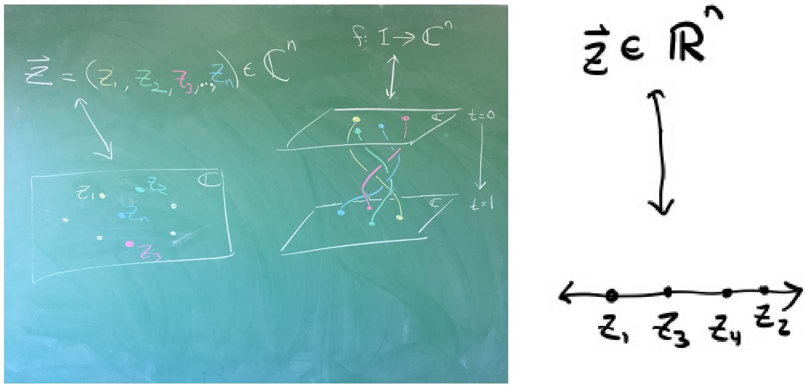

FIGURE 2. A single point in $\mathbb{C}^d$ can be viewed as d labeled points in $\mathbb{C}$, and a loop in $\mathbb{C}^d$ can be viewed as a pure braid. Similarly, a single point in $\mathbb{R}^d$ can be viewed as d labeled points in $\mathbb{R}$.

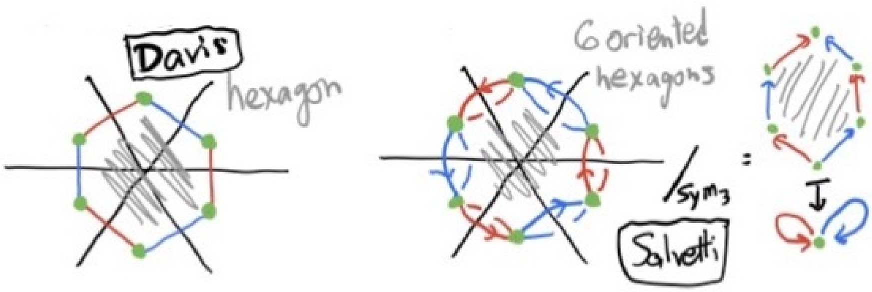

FIGURE 3. The cell structure dual to the real braid arrangement is a permutaherdon, also known as the Davis complex for symmetric group. A modified version with orientations is the Salvetti complex for the braid group.

known as a permutahedron, and this is also the Davis complex for the symmetric group (with a slightly different cell structure). There is a modified version of this complex with orientations, the pure Salvetti complex, which is homotopy equivalent to the complex braid arrangement complement. Each polytopal face is replaced by one or more oriented faces, one for each vertex in the face. As shown in Figure 3, the six vertices, six edges and single hexagon that form the Davis complex are replaced by six vertices, twelve oriented edges and six oriented hexagons in the oriented Davis complex. The SYM_3-action on this new complex is free and the quotient has one vertex, two edges and one hexagon, giving the presentation 2-complex for the standard presentation of the 3-strand braid group: $\langle a, b \mid aba = bab \rangle$. See **[Par14, McC17]** for details.

The version with the reals restricted to a closed interval is also of interest, since it illustrates one way in which orthoschemes arise in nature.

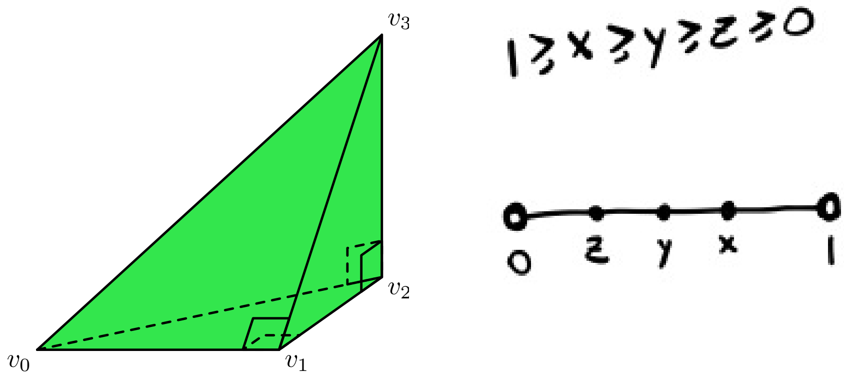

FIGURE 4. The interior of the standard 3-orthoscheme shown on the left can be described as the set of 3 distinct unlabeled points in the open interval $(0,1)$.

Remark 1.6. — If $\mathbb{I} = [0,1] \subset \mathbb{R}$, then $\mathbb{I}^d$ is an d-dimensional cube, and the quotient by the (non-free) SYM_d-action is a metric shape $\mathrm{SYM}_d \backslash \mathbb{I}^d$ that Tom Brady and I call a *standard unit d-orthoscheme* [**BM10**]. See Figure 4. If the labeled points are the interior of $\mathbb{I}$ and the single point in $\mathbb{I}^d$ avoids the real braid arrangement, the quotient space is the interior of the orthoscheme.

2. The Dual Braid Complex

The standard presentation of the braid group has a base configuration where the points are in a line along the real axis. The dual presentation, first defined by Birman, Ko and Lee in 1998, instead arranges the points at the d-th roots of unity around the unit circle, or equivalently, as the vertices of a convex polygon [**BKL98**]. This leads to a dual presentation and a dual Garside structure [**Bra01, Bes03**]. The dual simple generators are indexed by noncrossing partitions.

Definition 2.1. — A partition of the vertices of a convex d-gon is a *noncrossing partition* if the convex hulls of the blocks are pairwise disjoint. The set of all noncrossing partitions, ordered by refinement, forms a lattice called NC_d. This was first introduced by Kreweras and this lattice is closely connected to the dual presentation of the braid group [**Kre72, McC06**]. The Hasse diagram of NC_3 is shown on the lefthand side of Figure 5.

Definition 2.2. — Noncrossing partitions lead to *dual simple braids* (where the points move counter-clockwise around the convex hulls of the block of the partition), and the dual simple braids are part of the dual Garside structure. The Garside element is the d-cycle which rotates the vertices of the d-gon, and the atoms are the set of $\binom{d}{2}$ half-twists.

Remark 2.3. — Given a Garside structure, there is a standard construction of a classifying space [**CMW04**]. Its universal cover is a simplicial complex whose 1-skeleton is the Cayley

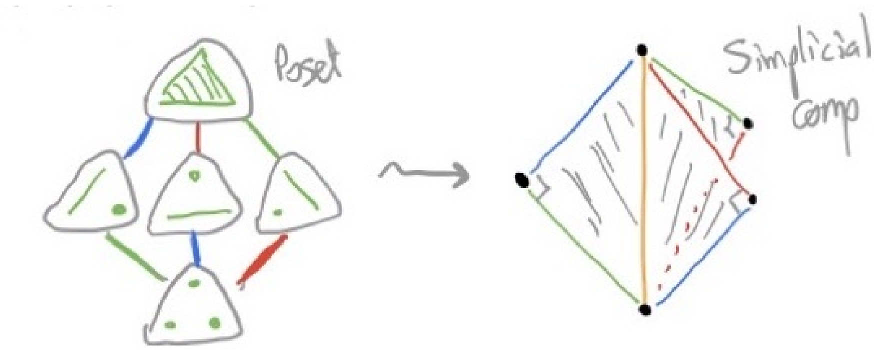

FIGURE 5. The noncrossing partition lattice and its geometric realization with the orthoscheme metric.

graph of the Garside group with respect to the simple generators. The classifying space itself is the one-vertex quotient of this universal cover by the simplicial group action. Note that the quotient is a Δ-complex, in the sense of Hatcher, rather than a (oriented) simplicial complex [**Hat02, DMW20**]. The standard construction applied to the dual Garside structure for the braid groups is the *dual braid complex*, and the geometric realization of NC_d is a strong fundamental domain from the BRAID_d-action on the universal cover of the dual braid complex. In [**BM10**], Tom Brady and I add a piecewise Euclidean metric to this complex by turning each simplex into an orthoscheme.

***Remark 2.4.* —** Also in [**BM10**], Tom and I conjecture that the dual braid complex with the orthoscheme metric is always locally $\mathrm{CAT}(0)$ and this has been shown when the number of strands is very small [**BM10, HKS16**]. The present work is part of a new approach to proving this theorem for all of the braid groups, by placing the dual braid complex inside the higher dimension critical value complex.

And finally, here is an illustration of how this works in an easy-to-visualize low-dimensional example.

***Example 2.5.* —** The dual presentation is for the braid group on 3-strands is:

$$\mathrm{BRAID}_3 = \langle a, b, c, d \mid ab = bc = ca = d \rangle$$

The universal cover of the dual braid complex is a metric trivalent tree cross $\mathbb{R}$ and the orthoscheme realization of the NC_3 poset is a strong fundamental domain for the vertex-transitive BRAID_3-action. The one-vertex quotient is the presentation 2-complex for the dual presentation. The noncrossing partition lattice and its geometric realization with the orthoscheme metric are shown in Figure 5. A portion of the corresponding universal cover is shown in Figure 6 and a copy of the orthoscheme realization of NC_3 has been outlined.

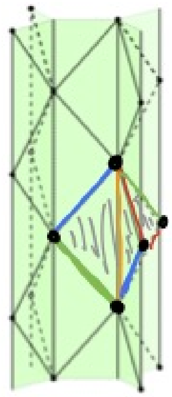

FIGURE 6. A portion of the (universal cover of the) dual braid complex with $d = 3$. Metrically, it is a trivalent tree cross $\mathbb{R}$ and the orthoscheme realization of the NC_3 poset is a strong fundamental domain for the vertex-transitive BRAID_3-action.

3. The Critical Value Complex

Since the two sequences of spaces described in Sections 1 and 2 are classifying spaces for the same sequence of groups, we know abstractly that they are homotopy equivalent. It has been difficult, however, to find a natural way to make this connection more concrete. Over the years, I tried, with various collaborators, to define an embedding of the dual braid complex into the symmetric quotient of the complex hyperplane complement so that it is at least linear on each simplex, even if it does not preserve the edge lengths and the orthoscheme metric. This can be done for $d = 3$, but our attempts would always fail for $d > 3$.

Then, in 2017, I gave a talk at Patrick Dehornoy's retirement conference in Caen where I mentioned this problem in passing. On the train ride back to Paris, Daan Krammer explained to me an approach that (1) gives a natural way to embed the dual braid complex into the classical classifying space, and (2) explains the origin of the orthoscheme metric in this context. The solution is to view points in the classical classifying space as polynomials(!) and then to take these polynomials seriously. The conversion to polynomials is straight-forward and classical.

***Definition 3.1.* —** The quotient of the complex hyperplane complement $Y = \mathrm{SYM}_d \backslash (\mathbb{C}^d - \mathcal{H})/\mathbb{C}\mathbf{1}$ can be identified with the space of monic degree d complex polynomials with distinct (unlabeled) roots up to (precomposition by) translation. Concretely, a point in Y is realized as d unlabeled points in $\mathbb{C}$ and then these are turned into the roots of the polynomial.

Once the points in Y are thought of as polynomial maps from $\mathbb{C}$ to $\mathbb{C}$, one can consider their critical points and critical values. In this language, here is the theorem which Krammer roughly stated in 2017 and which Michael and I are proving.

Theorem 3.2. **—** *Let Y be the space of monic complex polynomials of degree d with distinct unlabeled roots up to precomposition with translations. The subspace of polynomials where all of its critical values lie on the unit circle is homeomorphic to the dual braid complex. Moreover, there is a natural metric on this subspace defined by how the critical values move around the unit circle as the polynomial varies, and this defines the orthoscheme metric.*

Actually, what Michael and I are proving is somewhat stronger [**DMb**]. We define a bounded metric on all of Y, not just the subspace of polynomials with critical values on the unit circle, and turn the metric completion of Y into finite piecewise Euclidean cell complex.

Theorem 3.3. **—** *There is a natural bounded metric on the open manifold Y so that its metric completion, which we call X, is a compact space which supports a natural piecewise Euclidean cell structure.*

The cell complex X described in Theorem 3.3 is what we call the *critical value complex*.

Remark 3.4. **—** In [**DMb**] we also prove that the dual braid complex isometrically embeds into the critical value complex and there is a deformation retraction from the critical value complex onto the image of the dual braid complex. The proof uses a technical result that we proved in [**DM20**]. In [**TBY⁺20**], William Thurston and his co-authors also prove a version of this retraction, but in a completely different language and without realizing that the space to which it deformation retracts is the dual braid complex. They refer to this space as the "space of principal d-majors".

Here is another typical result that our methods allow us to prove.

Theorem 3.5. **—** *The subspace of polynomials where all critical values lie in a fixed closed subinterval of the positive real axis is contractible, and as a metric object it is the orthoscheme realization of the noncrossing partition lattice NC_d.*

In other words, there is an orthoscheme realization of NC_d coming from polynomials all of whose critical values lie on a ray out of the origin, and there is a second orthoscheme realization of NC_d (with face identifications forming the dual braid complex) coming from polynomials all of whose critical values lie on the unit circle. The full critical value complex is a subdirect product of these two piecewise Euclidean cell complex and the result is a manifold with boundary.

I would like to highlight the concrete and explicit nature of the cell structure in the critcial value complex. In the critical value complex there are $d^{d-2} \cdot n!$ top-dimensional cells indexed by a maximal chain in NC_d and a permutation in $\textsc{Sym}_n$, where $n = d - 1$. Each such cell is the direct product of two n-dimensional orthoschemes. Here is a rough description of the critical value complex for $d = 2$, 3 and 4.

Example 3.6. **—** When $d = 2$, the cell structure on X is an annulus built out of $2^0 \cdot 1! = 1$ rectangle (a 2-polytope) by gluing a pair of opposite sides. When $d = 3$, the cell structure on X is the union of $3^1 \cdot 2! = 6$ 4-polytopes, each of which is a right-angled triangle cross a right-angled triangle (i.e. the product of two 2-orthoschemes). When $d = 4$, the cell structure on X is the union of $4^2 \cdot 3! = 96$ 6-polytopes, each of which is a direct product of two 3-orthoschemes.

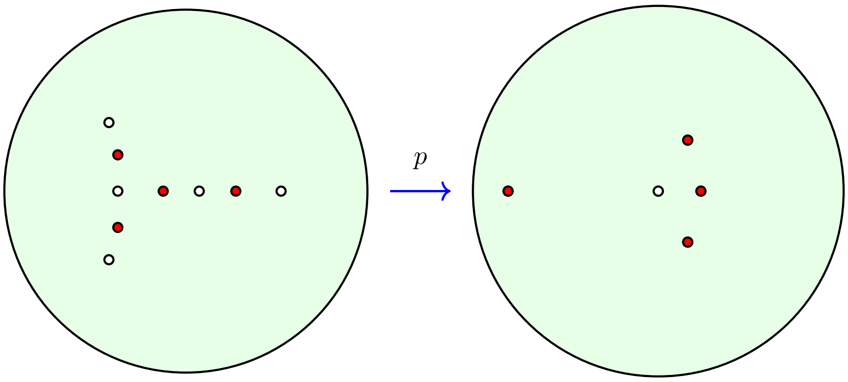

FIGURE 7. The roots, critical points and critcal values of our standard example. The lefthand side shows the five roots in white and the four critical points in red. The righthand side shows the four critical values in red and the origin in white.

The critical value complex is a new metric classifying space for the braid group and its geometric structure has not previously been studied. One conjecture that Michael and I have not yet been able to prove, but which we firmly believe, is that the critical value complex is exactly as non-positively curved as the dual braid complex inside it.

Conjecture 3.7. — *The critical value complex is* $\mathrm{CAT}(0)$ *for a particular value of* d *iff the dual braid complex is* $\mathrm{CAT}(0)$ *for that value of* d.

4. The Polynomial Viewpoint

In order to explain how the polynomial viewpoint leads to the theorems listed in Section 3, it is useful to look at the structure of a single polynomial map p from $\mathbb{C}$ to $\mathbb{C}$. In [**DMa**], Michael and I construct a genus 0 surface with a $\mathrm{CAT}(0)$ rectangular tiling for each complex polynomial with distinct roots. Note that most of this section focuses on a single polynomial, which merely represents a point in the complex hyperplane complement. A few remarks at the end of the section describe how these local structures lead to a metric and a cell structure as the polynomial varies.

Definition 4.1. — Let $p(z)$ be a degree-d complex polynomial viewed as a map from $\mathbb{C}$ to $\mathbb{C}$. There are three (multi)sets of points associated with p, namely its roots, critical points and critical values. The roots of p are the preimage of 0, the critical points are the roots of p' and the critical values are the images of the critical points. Note that the roots and critical points are in the domain, while the critical values are in the range.

Throughout this section we use the following standard example.

Example 4.2. — Consider the polynomial $p(z) = 3z^5 - 15z^4 + 20z^3 - 30z^2 + 45z$ with derivative $p'(z) = 15(z^2+1)(z-1)(z-3)$. The roots, critical points and critical values of p are shown in Figure 7. The lefthand side shows the five roots in white and the four critical

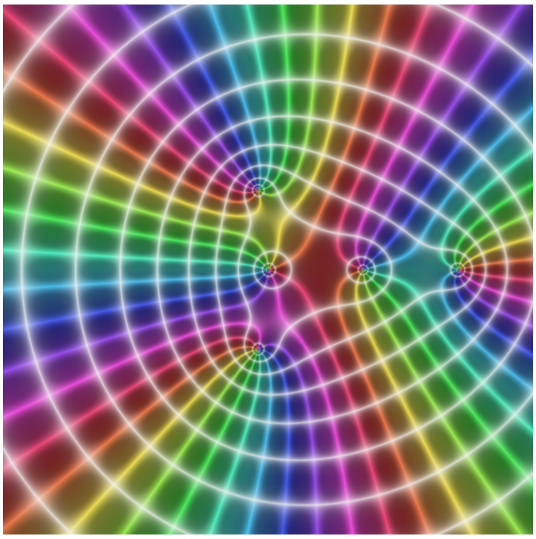

FIGURE 8. A tiled diagram for our standard example produced by Steve Trettel using Mathematica. The roots are located where all the colored lines converge and the critical points are located in the regions that are not twisted topological rectangles.

points in red. The righthand side shows the four critical values in red and the origin in white. Note that slightly different scales have been used in the domain and range.

Recall that the location of the critical values determines whether the roots are distinct.

***Lemma 4.3.* —** *For a complex polynomial $p(z)$, the following are equivalent: (1) p has no repeated roots, (2) the roots and critical points are disjoint sets, and (3) the critical values of p are all nonzero.*

Next, recall how tiled diagrams can be used to encode and display functions from $\mathbb{C}$ to $\mathbb{C}$.

***Remark 4.4.* —** The idea behind a tiled diagram is to color and shade the points in the range based on the argument and magnitude of their image. In particular, the points in the range are assigned colors based on their argument and a shade based on their magnitude. The points in the domain are then colored and shaded so that the map p is color and shade preserving. If only certain arguments and magnitudes are drawn, the result looks like a twisted rectangular tiling with a few exceptional 2-cells. Figure 8 shows a tiled diagram for our standard example polynomial as produced by Mathematica.

When p has distinct roots, all of the crucial information about critical points and critical values is contained in the restricted map $p_{\mathbf{0}}: \mathbb{C}_{\mathbf{rts}} \to \mathbb{C}_{\mathbf{0}}$, with the roots removed from the domain and the origin removed from the range.

***Definition 4.5.* —** We assign a bounded metric to the once punctured plane $\mathbb{C}_{\mathbf{0}}$, by first mapping it to the twice punctured sphere via stereographic projection, and then radially projecting

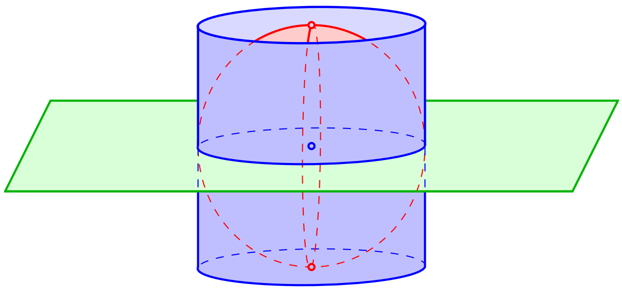

FIGURE 9. The three spaces described in Remark 4.5.

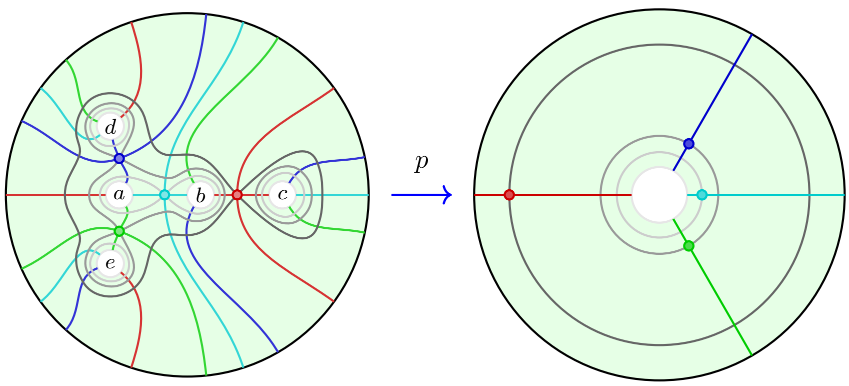

FIGURE 10. The branched annulus for our standard example, with its metric rectangular tiling.

it to the open annulus cylinder $\mathbb{T} \times \mathbb{I}^{\text{int}}$. See Figure 9 where the plane, sphere and vertical annulus are shown in green, red and blue, respectively. Note that rays and circles in the plane $\mathbb{C}_{\mathbf{0}}$, defined by constant argument or constant magnitude, correspond to longitudes and latitudes in the sphere $\mathbb{S}^2$ and to horizontal circles and vertical lines in the vertical annulus $\mathbb{T} \times \mathbb{I}$. In [**DMa**] we extend the longitude and latitude language to all three spaces.

Definition 4.6. — Once we impose the bounded annulus metric to the range of $p_{\mathbf{0}}$, there is a unique pullback metric on the domain which makes this map a local isometry everywhere except at the isolated critical points around which it is branched. Moreover, so long as p has more than one root, there is at least one critical point and at least one nonzero critical value, and these can be used to give a metric rectangular structure to the (closure of the) vertical annulus. This metric cell structure also pulls back through p to define a nonpositively curved metric rectangular tiling of a genus 0 surface that we associate to the polynomial p. We call this the *branched annulus* of p. A planar drawing of the branch annulus of our standard example is shown in Figure 10. Keep in mind, however, that every twisted rectangle shown is, in fact, a metric Euclidean rectangle with a metric determined by the corresponding metric rectangle in metric rectangular tiling of the vertical annulus.

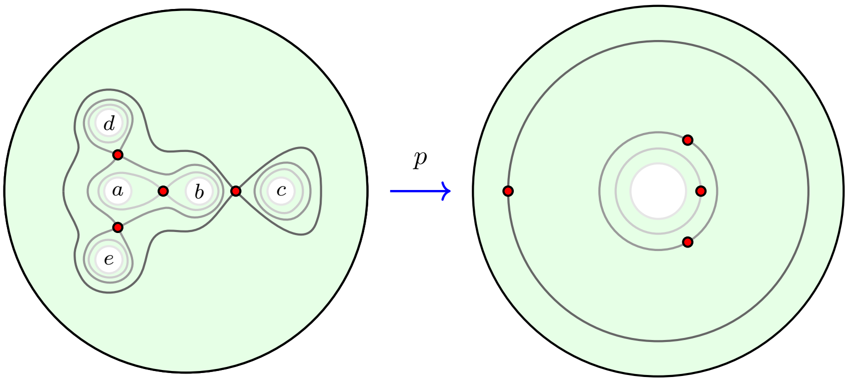

FIGURE 11. The regular and critical latitudes in our standard example determines the following chain in the partition lattice: $\{a, b, c, d, e\} \subset \{ab, c, d, e\} \subset \{abde, c\} \subset \{abcde\}$.

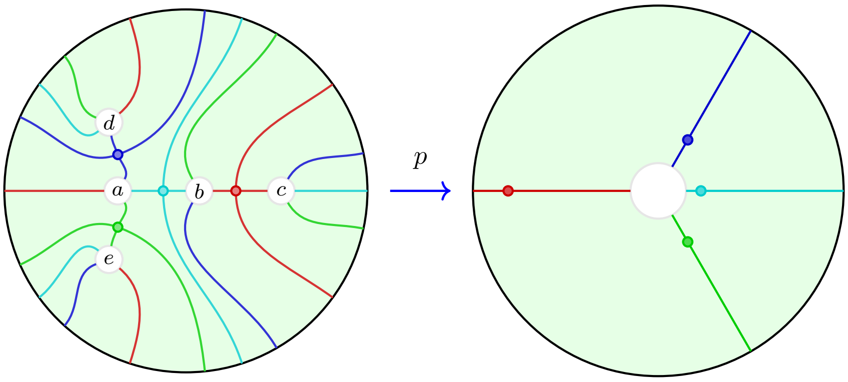

FIGURE 12. The preimage of all of the critical longitudes for our standard example. This structure can be encoded in a factorization of a d-cycle.

The preimages of the longitudes and latitudes in annulus carry detailed information about the structure of the branched annulus and this can be encoded in various combinatorial objects.

Definition 4.7. **—** A horizontal circle in the vertical annulus is a *critical latitude* if it contains a critical point of p, and it is regular otherwise. The preimages of regular latitudes are unions of circles, whereas the preimages of critical latitudes have some singular component with a structure called a *metric cactus*. As one transitions from the bottom of the annulus to the top, the preimages go from the d distinct root circles at the bottom to one big circle at the top. The order in which these root circles join up can be encoded in a chain inside the partition lattice on the roots. Our standard example determines the following chain in the partition lattice: $\{a, b, c, d, e\} \subset \{ab, c, d, e\} \subset \{abde, c\} \subset \{abcde\}$. See Figure 11.

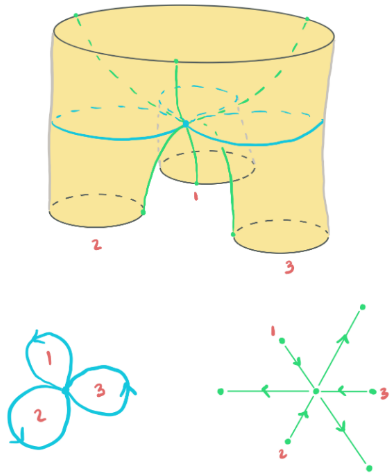

FIGURE 13. An example of a multipedal pair of pants with 3 legs. It has only one critical point and one critical value. Its unique metric cactus and unique metric banyan are shown at the bottom of the figure.

Definition 4.8. — A vertical line in the vertical annulus is a *critial longitude* if it contains a critical point of p, and it is regular otherwise. The preimages of regular longitudes are unions of d noncrossing lines connecting d root circles to the single boundary circle, whereas the preimages of critical longitudes have some singular component with a structure called a *metric banyan*. The structure of the preimages of the critical and regular longitudes can be encoded in a factorization of a d-cycle. See [**DMa**] for details.

Remark 4.9. — There is another, more vivid, 3-dimensional way to view the structure of the branched annulus. See Figure 13. Here the points have been arranged so that their heights correspond to the height of their image in the vertical annulus. The result is a multipedal pair of pants with as many "legs" as there are roots. The figure show the multipedal pants for the cubic polynomial $p(z) = z^3 - 1$. A similar diagram for our standard example would have 5 "legs" which join up at various heights.

Our detailed structural results about branched annuli with their metric cacti and metric banyans can be found in [**DMa**]. And finally, a brief description indicating how these structures associated with individual polynomials, lead to a metric and a cell structure on a space constructed from the quotient of the complex hyperplane complement.

Remark 4.10. — The branched annulus of a polynomial p is constructed by pulling back a metric and a cell structure from the subdivided annulus in the range to form a branched annulus out of the domain. For the space $Y = \mathrm{SYM}_d \backslash (\mathbb{C}^d - \mathcal{H})/\mathbb{C}\mathbf{1}$ we do something very similar. There is a natural map from Y to $\mathrm{SYM}_n \backslash \mathbb{A}^n$, the space of multisets of $n = d - 1$ points in the vertical annulus. The map sends (the equivalence class of) the polynomial p to its multiset of critical values in $\mathbb{A}$. The quotient by $\mathbb{C}\mathbf{1}$ in the domain has been included precisely because precomposition with a transition changes the locations of the critical points, but it leaves the locations of the critical values unchanged. Moreover, a quick dimension count shows that Y and $\textsc{Sym}_n \backslash \mathbb{A}^n$ have the same dimension. In fact, the natural metric on $\textsc{Sym}_n \backslash \mathbb{A}^n$ determines a pullback metric on Y which makes the map a local isometry on a dense subspace. In addition, there is a natural cell structure on $\textsc{Sym}_n \backslash \mathbb{A}^n$. First, view $\mathbb{A}$ as an annulus formed by gluing a pair of opposite sides of a 2 by 2π rectangle. The space $\mathbb{A}^n$ can then be viewed as the product of an n-dimensional cube of side length 2 and an n-dimensional cube of side length 2π with some face identifications. The action of $\textsc{Sym}_n$ on this space (which unlabels the points in $\mathbb{A}$) is the diagonal action the product of these two n-cubes. We subdivide each n-cube into $n!$ orthoschemes, making $\mathbb{A}^n$ a space built out of $(n!)^2$ polytopes, each isometric to product of a standard n-orthoscheme of side length 2 and a standard n-orthoscheme of side length 2π. The quotient has $n!$ of these polytopes glued together according to the Hasse diagram of the weak Bruhat order on $\textsc{Sym}_n$. This cell structure also pulls back and induces a finite cell structure on (the metric completion of) Y. The results in [**DM20**] are the key technical tools that we use to make this precise.

Acknowledgements. — I would like to thank Daan Krammer for our conversation on the train to Paris in 2017. Even though he had never written up a proof for publication, Daan knew how to embed the dual braid complex into the quotient of the complex hyperplane complement using polynomials. Michael Dougherty and I have gone on to develop several articles worth of material inspired by this initial insight. Next, of course, I would like to thank Michael for our on-going collaboration. He has quickly shifted from being a former advisee to one of my regular co-authors. And finally, a very special thank you to Ruth Charney for all that she has done for the field as a whole. The way she interacts with those around her is always welcoming and encouraging. I would particularly like to thank her for a conversation in the late 1990s, which had a major positive impact on me personally, as I was attempting to re-engage with mathematical research after several years where I was only focusing on teaching.

Références

[Art25] Emil Artin, *Theorie der Zöpfe*, Abh. Math. Sem. Univ. Hamburg **4** (1925), no. 1, 47–72. MR 3069440

[Art47] E. Artin, *Theory of braids*, Ann. of Math. (2) **48** (1947), 101–126. MR 19087

[Bes03] David Bessis, *The dual braid monoid*, Ann. Sci. École Norm. Sup. (4) **36** (2003), no. 5, 647–683. MR 2032983

[BKL98] Joan Birman, Ki Hyoung Ko, and Sang Jin Lee, *A new approach to the word and conjugacy problems in the braid groups*, Adv. Math. **139** (1998), no. 2, 322–353. MR 1654165

[BM10] Tom Brady and Jon McCammond, *Braids, posets and orthoschemes*, Algebr. Geom. Topol. **10** (2010), no. 4, 2277–2314. MR 2745672

[Bra01] Thomas Brady, *A partial order on the symmetric group and new $K(\pi, 1)$'s for the braid groups*, Adv. Math. **161** (2001), no. 1, 20–40.

[BS72] Egbert Brieskorn and Kyoji Saito, *Artin-Gruppen und Coxeter-Gruppen*, Invent. Math. **17** (1972), 245–271. MR 48 #2263

[CMW04] R. Charney, J. Meier, and K. Whittlesey, *Bestvina's normal form complex and the homology of Garside groups*, Geom. Dedicata **105** (2004), 171–188. MR 2057250

[Dav08] Michael W. Davis, *The geometry and topology of Coxeter groups*, London Mathematical Society Monographs Series, vol. 32, Princeton University Press, Princeton, NJ, 2008. MR 2360474

[DDD+15] Patrick Dehornoy, François Digne, François Digne, Eddy Godelle, Daan Krammer, and Jean Michel, *Foundations of Garside theory*, EMS Tracts in Mathematics, vol. 22, European Mathematical Society (EMS), Zürich, 2015, Author name on title page: Daan Kramer. MR 3362691

[Del72] Pierre Deligne, *Les immeubles des groupes de tresses généralisés*, Invent. Math. **17** (1972), 273–302. MR 0422673 (54 #10659)

[DMa] Michael Dougherty and Jon McCammond, *Geometric combinatorics of polynomials I: the case of a single polynomial*, To appear in the *J. of Algebra*.

[DMb] ———, *Geometric combinatorics of polynomials II: the critical value complex*, In preparation.

[DM20] ———, *Critical points, critical values, and a determinant identity for complex polynomials*, Proc. Amer. Math. Soc. **148** (2020), no. 12, 5277–5289. MR 4163840

[DMW20] Michael Dougherty, Jon McCammond, and Stefan Witzel, *Boundary braids*, Algebr. Geom. Topol. **20** (2020), no. 7, 3505–3560. MR 4194287

[Gar69] F. A. Garside, *The braid group and other groups*, Quart. J. Math. Oxford Ser. (2) **20** (1969), 235–254. MR 248801

[Hat02] Allen Hatcher, *Algebraic topology*, Cambridge University Press, Cambridge, 2002. MR 1867354

[HKS16] Thomas Haettel, Dawid Kielak, and Petra Schwer, *The 6-strand braid group is* $\mathrm{CAT}(0)$, Geom. Dedicata **182** (2016), 263–286. MR 3500387

[Kre72] G. Kreweras, *Sur les partitions non croisées d'un cycle*, Discrete Math. **1** (1972), no. 4, 333–350. MR 309747

[McC06] Jon McCammond, *Noncrossing partitions in surprising locations*, Amer. Math. Monthly **113** (2006), no. 7, 598–610. MR 2252931

[McC17] ———, *The mysterious geometry of Artin groups*, Winter Braids Lect. Notes **4** (2017), no. Winter Braids VII (Caen, 2017), Exp. No. 1, 30. MR 3922033

[Par14] Luis Paris, *Lectures on Artin groups and the* $K(\pi, 1)$ *conjecture*, Groups of exceptional type, Coxeter groups and related geometries, Springer Proc. Math. Stat., vol. 82, Springer, New Delhi, 2014, pp. 239–257. MR 3207280

[Sal87] M. Salvetti, *Topology of the complement of real hyperplanes in* $\mathbf{C}^N$, Invent. Math. **88** (1987), no. 3, 603–618. MR 884802

[TBY+20] William P. Thurston, Hyungryul Baik, Gao Yan, John H. Hubbard, Kathryn A. Lindsey, Lei Tan, and Dylan P. Thurston, *Degree-d-invariant laminations*, What's next?—the mathematical legacy of William P. Thurston, Ann. of Math. Stud., vol. 205, Princeton Univ. Press, Princeton, NJ, 2020, pp. 259–325. MR 4205644

January 31, 2022

JON MCCAMMOND